Nitrate sources and dynamics in the salinized river and estuary- A $\delta^{15}N$- and $\delta^{18}O$-NO_3^- isotope approach

D. Xue[1], P. Boeckx[3], Z. Wang[1,2,*]

[1]Tianjin Key Laboratory of Water Resources and Environment, Tianjin Normal University, Tianjin 300387, China.

[2]State Key Laboratory of Environmental Geochemistry, Institute of Geochemistry, Chinese Academy of Sciences, Guiyang 550002, China.

[3]Isotope Bioscience Laboratory - ISOFYS, Faculty of Bioscience Engineering, Ghent University, Coupure links 653, 9000 Ghent, Belgium.

*Correspondence to:

Zhong-Liang Wang, Tianjin Key Laboratory of Water Resources and Environment, Tianjin Normal University, Tianjin 300387, China.

E-mail: wangzhongliang@vip.skleg.cn

Tel.and fax: +86 22 237666256

Abstract

To trace NO_3^- sources and assess NO_3^- dynamics in the salinized rivers and estuaries, three rivers (HH River, CB River and JY River) and two estuaries (HH Estuary and CJ Estuary) along the Bohai Bay (China) have been selected to determine DIN and $\delta^{15}N$- and $\delta^{18}O$-NO_3^-. Upstream of the HH River NO_3^- was removed 30.9±22.1% by denitrification, resulting from effects of the floodgate: limiting water exchange with downstream and prolonging water residence time to remove NO_3^-. Downstream of the HH River NO_3^- was removed 2.5±13.3% by NO_3^- turnover processes. Conversely, NO_3^- was increased 36.6±25.2% by external N source addition in the CB River and 34.6±35.1% by in-stream nitrification in the JY River, respectively. The HH and CY Estuaries behaved mostly conservative excluding the sewage input in the CJ Estuary. Hydrodynamic in estuaries has changed by the ongoing reclamation projects, aggravating the estuary losing the attenuation function of NO_3^-.

Key words: N pollution, estuary mixing, source and sink, NO_3^- dynamic, $\delta^{15}N$- and $\delta^{18}O$-NO_3^-, floodgate

1. Introduction

Increasing population, extensive agricultural activities and rapid development of urbanization in coastal areas have dramatically increased N loading to rivers and coastal waters (Seitzinger and Kroeze 1998; Jennerjahn et al., 2004; Umezawa et al., 2008). Estuaries play a prominent role for delivery of terrestrially derived N to coastal water through physical, chemical, and biological processes (Mulholland 1992; Bernhardt et al. 2003; Sebilo et al. 2006; Hartzell and Jordan, 2012).

Many estuarine studies have focused on tracing N sources and assessing N dynamics in large estuarine systems, such as the Elbe Estuary (Dähnke et al., 2008) and the Atlantic coast (Middelburg and Herman, 2007) in Europe, the San Francisco Bay Estuary (Wankel et al., 2006), the Mississippi River Estuary (Rabalais et al.,1996), and the Mid-Atlantic coast (Dafner et al., 2007) in the United States, and the Yangtze River Estuary (Chai et al., 2009) and Pearl River Estuary (Dai et al., 2008) in China. Compared to these large estuarine systems with high discharge of freshwater, the levels of freshwater discharge are relatively low in the small estuaries, which are characterized by salinization from sea-water intrusion for rather long distances upstream (Graas and Savenije, 2008). How do these salinized estuaries respond to increased N loading? How do physical and biological processes control DIN (NH_4^+, NO_2^- and NO_3^-) concentration variations?

To answer these questions, an intensive study was conducted in three rivers and the corresponding estuaries characterized by different levels of salinization in a coastal municipality (Tianjin) along the Bohai Bay (China). Two investigated rivers with mean salinities around 0.5 and 0.7 flow through a rural area and converge before entering into the estuary. The third one with mean salinity around 2.2 flows through Tianjin municipality and is separated into three parts by two floodgates crossing the

river, for providing water supply for the residents living along the river bank. Since the rapid urbanization and population growth in Tianjin municipality, NO_3^- loading progressively increased in rivers and estuaries associated with human activities, such as agricultural runoff, untreated domestic and industrial wastewater (Gao et al., 2011). Furthermore, port constructions and reclamation projects along the coastline of the municipality even aggravate NO_3^- pollution (Zhang et al., 2004). Thus, tracing NO_3^- sources and assessing NO_3^- dynamics in the salinized rivers and estuaries represent fundamental goals in this study.

More than concentration data alone, the combined use of N ($\delta^{15}N$) and O ($\delta^{18}O$) isotopes of NO_3^- has provided a powerful tool to investigate NO_3^- dynamics and identify NO_3^- sources in estuaries (Middelburg and Nieuwenhuize 2001; Sebilo et al. 2006; Wankel et al. 2006; Dähnke et al., 2008; Miyajima et al., 2009). Therefore, in the present study, a combined approach based on the mixing curves of DIN concentration versus salinity and $\delta^{15}N$- and $\delta^{18}O$-NO_3^- is applied to (1) identify potential dominant NO_3^- sources responsible for NO_3^- contamination; and (2) elucidate possible NO_3^- dynamics in the different salinized rivers and the estuaries.

2. Material and method

2.1 Study area

The investigated three rivers are located in a coastal municipality, Tianjin, China (Fig. 1). The study region is influenced by the warm temperate semi-humid monsoon climate with an average annual temperature of 11.4–12.9˚C. The annual precipitation is 520–660 mm, with 75% of the total precipitation occurring in June, July and August (yue et al., 2010). The population of Tianjin municipality is ca.16 million and the density is 1100 inhabitants km^{-2}. The survey took place in the dry season for three

rivers along a salinity gradient, the Haihe River (HH River) on 7 Nov. 2012, the Chaobaixin River (CB River) on 9 Nov. 2012 and the Jiyun River (JY River) on 10 Nov. 2012 (Fig.1). Water samples were also taken along the estuary of the HH River (HH Estuary) and the mixing estuary of the CB River and the JY River (CJ Estuary) on 16 Nov. 2012 to study reactive N transformation processes from the river to the estuary (Fig.1). The HH River is characterized by 72km in length, ca. 100m in width, 3-5m in depth, and a watershed area of 2066 km^2 (Liu et al., 2001). Since the separation by the floodgate F1, the upstream part of the HH River serves as a river-type reservoir for the purpose of supplying water to the residents living along the river bank. The other floodgate F2 is located at the end of the HH River serves as flood discharging, tidal blocking and ship traffic. Although there were eight sewage outlets along the HH River, they were all forbidden to discharge. The average runoff of the HH River is 12.36×10^8 m^3/a; the average tidal amplitude is 2.43 m; and the average flow velocity is 0.3-0.4 m/S in 2000-2004 (Wen and Xing, 2004). The CB River flows through a rural area and is characterized by 81km in length, ca. 700 m in width, 5-7m in depth, and a watershed area of 1387 km^2 (Gburek and Sharpley, 1998). Animal manure could be a potential dominant NO_3^- source in the CB River as this watershed has important livestock breeding base for the municipality (Shao et al., 2010). The JY River flows through agricultural area and is considered as a significant water source for agricultural and domestic use. The JY River is characterized by 144km in length, ca. 300 m in width, less than 7 m in depth, and a watershed area of 2146 km^2(Chen et al., 2000). The average runoff of the converged river mouth of the CB River and the JY River is 16.03×10^8 m^3/a; the average tidal amplitude is 2.45m; and the average flow velocity is 0.5-0.7 m/S in 1990-1997(Liang and Xing,1999). Unfortunately, we have no hydrological data for these rivers during the study period.

126
127 2.2 Sampling and analysis

128 Water samples were taken on a bridge using a bucket serially from upstream
129 downwards for the rivers and on a ship for estuarine water. The bucket was put into
130 the river/estuary water until it reached ~0.5m below the surface to sample water.
131 Water samples were stored frozen in 1L HDPE (High Density Polyethylene) bottles
132 for determination of physico-chemical properties and $\delta^{15}N$- and $\delta^{18}O$-NO_3^-. Salinity,
133 temperature (T), pH and dissolved oxygen (DO) were measured by a portable water
134 quality probe (Thermo Orion, USA). Laboratory analyses included NO_3^-, NO_2^- and
135 NH_4^+. All samples were filtered through 0.45 μm membrane filters and stored at 4˚C
136 until analysis. Nitrate (NO_3^-), NO_2^- and NH_4^+ concentrations were analyzed on a
137 continuous flow analyzer (Auto Analyzer 3, Seal, Germany).

138 The $\delta^{15}N$- and $\delta^{18}O$-NO_3^- values were determined by the "Bacterial denitrification
139 method" (Sigman et al., 2001; Casciotti et al., 2002; Xue et al., 2010) in the UC Davis
140 Stable Isotope Facility of California University, which allows for the simultaneous
141 determination of $\delta^{15}N$ and $\delta^{18}O$ of N_2O produced from the conversion of NO_3^- by
142 denitrifying bacteria, which naturally lack N_2O - reductase activity. Isotope ratios of
143 $\delta^{15}N$ and $\delta^{18}O$ are measured using a Thermo Finnigan GasBench + PreCon trace gas
144 concentration system interfaced to a Thermo Scientific Delta V Plus isotope-ratio
145 mass spectrometer (Bremen, Germany). The N_2O sample is purged from vials through
146 a double-needle sampler into a helium carrier stream (25 mL/min) and CO_2 is
147 removed using scrubber (Ascarite). By cryogenic trapping and focusing, the N_2O is
148 compressed onto an Agilent GS-Q capillary column (30m x 0.32 mm, 40°C, 1.0
149 mL/min) and subsequently analyzed by IRMS.

150 Stable isotope data were expressed in delta (δ) units in per mil (‰) relative to the
151 respective international standards:

$$\delta_{sample}\,(‰) = \left(\frac{R_{sample}}{R_{standard}} - 1\right) \times 1000 \quad (1)$$

where R_{sample} and $R_{standard}$ are the $^{15}N/^{14}N$ or $^{18}O/^{16}O$ ratio of the sample and standard for $\delta^{15}N$ and $\delta^{18}O$, respectively. Values of $\delta^{15}N$ are reported relative to atmospheric air (AIR) and $\delta^{18}O$ values are reported relative to Vienna Standard Mean Ocean Water 2 (VSMOW 2). The calibration standards are the nitrates USGS 32, USGS 34, and USGS 35, and are supplied by NIST (National Institute of Standards and Technology, Gaithersburg, MD).

2.3 Mixing model

The concentration of a mixture can be calculated via a basic mixing model (Liss, 1976):

$$C_{MIX} = f \times C_R + (1 - f)\, C_M \quad (2)$$

where C represents concentration, the subscripts R and M represent riverine and marine end-members, respectively; f represents the fraction of freshwater in each sample calculated from salinity (Dähnke et al., 2008):

$$f = (salinity_{MAX} - salinity_{MEA}) / salinity_{MAX} \quad (3)$$

where MAX is taken as the maximum measured salinity of marine end-member for coastal water and MEA is taken as the measured salinity of the mixture.

Isotopic values of mixed estuarine samples (δ_{MIX}) were calculated using concentration-weighted isotopic values for riverine and marine end-members, respectively (Fry 2002; Dähnke, 2008):

$$\delta_{MIX} = [f \times C_R \times \delta_R + (1 - f) C_M \times \delta_M]/C_{MIX} \quad (4)$$

where C represents concentration, δ represents isotopic value, the subscripts R and M represent riverine and marine end-members, respectively; and f represents the fraction of freshwater in each sample. The salinity-based isotopic mixing does not follow

linear conservative mixing but show curvilinear mixing that reflects concentration-based weighting of end-member isotopic contributions.

When a conservative mixing appeared between the riverine and marine end-members, DIN distribution is expected to fall on the linear mixing line. When an enriched external source or biological transformation (e.g. mineralization, nitrification, etc.) contributes into the river, DIN distribution is expected to fall above the mixing line. In turn, when a depleted external source or the internal removal processes (e.g., denitrification, assimilation, etc.) appears in the river, DIN distribution is expected to fall below the mixing line (Wankel et al., 2006). The curvilinear mixing curves of determined $\delta^{15}N$ and $\delta^{18}O$ of NO_3^- provide better information for transformation processes: an isotopic enriched NO_3^- source or internal removal processes (e.g. denitrification, assimilation, etc.) will result in a distribution of $\delta^{15}N$ and $\delta^{18}O$ falling above the mixing lines, while an isotopic depleted nitrate source or internal nitrification will result in a distribution of $\delta^{15}N$ and/or $\delta^{18}O$ falling below the mixing line.

2.4 Nitrate removal efficiency

Variation percentages of the measured NO_3^- concentrations compared to that of the calculated mixing lines were computed to assess the NO_3^- removal efficiency for the rivers and estuaries as follows:

$$\text{Variation (\%)} = \frac{C_{measured} - C_{theoretical}}{C_{theoretical}} \times 100\% \quad (5)$$

where $C_{measured}$ represents the measured NO_3^- concentration; and $C_{theoretical}$ represents the theoretical NO_3^- concentration calculated based on the mixing line. A variation percentage > 0 represents a source; a variation percentage < 0 represents a sink; and a variation percentage equal to 0 represents a mixing.

202

203 3. Results

204 3.1 Physicochemical properties

205 Table 1 summarizes the data of physicochemical properties collected in this study in
206 the rivers and estuaries. Obviously, the salinities of the HH River (ranging from 0.7 to
207 4.9 with a mean value of 2.2) and its estuary (ranging from 18.6 to 24.1 with a mean
208 value of 21.2) is higher than the rivers of CB (ranging from 0.5 to 0.6 with a mean
209 value of 0.5) and JY (ranging from 0.6 to 0.8 with a mean value of 0.7) and the
210 corresponding estuary (ranging from 2.0 to 20.0 with a mean value of 7.7),
211 respectively. The municipality had been suffering multiple seawater intrusion and
212 regression, which results in the salinization of the rivers and soil (Wang, 2004), while
213 the greater salinization level of the HH River is also related to seawater intrusion over
214 the floodgate until upstream of the HH River in a relatively long distance. The rivers
215 and the estuaries showed similar pH values between 7.5 and 8.6. The temperature of
216 HH River varied around 12.3˚C slightly higher than the CB River (mean is 10.9˚C)
217 and the JY River (11.5˚C). The mean temperature of the HH Estuary (9.7) is also
218 higher than that of the CJ Estuary (6.7). Dissolved oxygen (DO) concentrations were
219 relatively enriched in this study (higher than 7.2 mg L^{-1}), excluding the DO depleted
220 area in the upstream of the HH River (lower than 5.0 mg L^{-1}).

221

222 3.2 DIN species

223 Wide concentration variations were noticeable for DIN (NH_4^+, NO_2^- and NO_3^-)
224 species in Table 1. In the HH River, the NH_4^+ concentrations varied from 124.1 to
225 332.6 μmol L^{-1}, the NO_3^- concentrations varied from 62.5 to 219.0μmol L^{-1} and the
226 NO_2^- concentrations varied from 7.2 to 20.8μmol L^{-1}. The DIN concentrations of the

HH Estuary varied smoothly (5.6-6.7 μmol L^{-1} for NO_2^-, 7.1-25.7 μmol L^{-1} for NO_3^-, and 65.7-88.1 μmol L^{-1} for NH_4^+) and were quite low compared to the HH River. Nitrate concentrations in the CB river were relatively elevated (120.0 – 171.5 μmol L^{-1}) with a continuous accumulation along the entire salinity gradient, while NO_2^- concentrations decreased from 12.0 to 6.0 μmol L^{-1}. Ammonium concentrations in the CB River varied from 143.9 to 380.0 μmol L^{-1}. The JY River also showed NO_3^- accumulation (increased from 40.0 to 83.3 μmol L^{-1}) along the entire salinity gradient, while a decreasing trend was observed for both NO_2^- (decreased from 7.0 to 2.1 μmol L^{-1}) and NH_4^+ (decreased from 72.8 to 11.1μmol L^{-1}) concentrations. The CJ Estuary displayed a sea-ward decreasing trend with relatively elevated concentrations in NH_4^+ (328.4-43.2 μmol L^{-1}), NO_2^- (7.8-3.4μmol L^{-1}) and NO_3^- (153.4-6.1 μmol L^{-1}). Compared to the other river and estuaries, DIN results of this study are similar to that in the Pearl River Estuary (Dai et al., 2008) in South China Sea, but higher than that in the Elbe Estuary (Dähnke et al., 2008) in Europe and the San Francisco Bay Estuary (Wankel et al., 2006) in the United States. The specific reasons to cause such variations could be potentially linking to internal/external N source contributions and different N dynamics in the rivers and the estuaries.

3.3 Isotopic composition of NO_3^-

The isotopic composition of NO_3^- varied spatially among the rivers and the estuaries (Table 1). The $\delta^{15}N\text{-}NO_3^-$ values in the HH River varied from -0.2 to 8.4‰ and the $\delta^{18}O\text{-}NO_3^-$ values varied from -0.5 to 1.5‰. The isotopic composition of NO_3^- in the HH Estuary remained stable around 8.1‰ for $\delta^{15}N\text{-}NO_3^-$ and 5.6‰ for the $\delta^{18}O\text{-}NO_3^-$. In the CB River, the $\delta^{15}N\text{-}NO_3^-$ values were enriched with a mean of 13.6‰, and the $\delta^{18}O\text{-}NO_3^-$ values were in a range between 3.9 and 5.6‰. A decrease in $\delta^{15}N\text{-}NO_3^-$

252 (from 6.5 to 4.4‰) and an increase in $\delta^{18}O\text{-}NO_3^-$ (from 0.8 to 5.3‰) values along the
253 salinity were observed in the JY River. The CY Estuary demonstrated a wide range of
254 $\delta^{15}N\text{-}NO_3^-$ (from 7.1 to 15.0‰), while a narrow range of $\delta^{18}O\text{-}NO_3^-$ (from 5.9 to
255 6.9‰).
256
257 4. Discussion
258 4.1 Potential dominant NO_3^- sources
259 To derive qualitative information on the predominant NO_3^- sources in the rivers and
260 the corresponding estuaries, a classical dual isotope approach ($\delta^{15}N\text{-}NO_3^-$ vs.
261 $\delta^{18}O\text{-}NO_3^-$) has been applied (Figure 2). It is clear that the isotope signatures of all the
262 sampling locations showed in a scattered distribution, indicating different NO_3^- source
263 influence in the rivers and the estuaries. Upstream of the HH River at a salinity of 1.0,
264 a floodgate F1 separates the river into two parts; and at the end of the river at the
265 salinity of 4.9, the other floodgate F2 controls the connection of the river to the HH
266 Estuary. Hence, the $\delta^{15}N$- and $\delta^{18}O\text{-}NO_3^-$ values of the HH River behaved quite
267 differently, which moved from the overlapping area of the "NH_4^+fertilzier"and "soil
268 N" source boxes for the majority of the upstream sampling locations, to the
269 overlapping area of the "soil N" and "manure and sewage" source boxes at the end of
270 the river. In this study, the majority of the sampling locations were potentially
271 influenced by the source of "soil N" or "sewage" not the "mineral fertilizer", as the
272 HH River flows through the municipality without agricultural activities. In addition, it
273 can no be excluded the influence from salt water intrusion from the estuary, which
274 showed similar isotopic values to that at the end of the HH River. The distribution of
275 the HH Estuary does not show a landward trend due to the floodgate F2 at the end of
276 the HH River, but falls into the range of marine NO_3^- reported by Kendall et al.

277 (2007).

278 Animal manure could be a potential dominant NO_3^- source in the CB River as this
279 watershed plays the role of important livestock breeding base for the municipality
280 (Shao et al., 2010). Furthermore, the $\delta^{15}N\text{-}NO_3^-$ values were enriched and varied
281 around 14‰, indicating anthropogenic NO_3^- derived from manure (Kendall et al.,
282 2007; Xue et al., 2009). The isotope signatures of the JY River were mainly
283 concentrated in the "soil N" source box. The $\delta^{15}N\text{-}NO_3^-$ and $\delta^{18}O\text{-}NO_3^-$ values of the
284 CJ Estuary suggested an influence of the CB River. In addition, quite high DIN
285 concentrations (Table 1) appeared in this estuary, due to sewage discharge of mooring
286 ships in the vicinity of the sampling area. Thus, the influence of sewage and the CB
287 River was considered as the dominant NO_3^- source.

288

289 4.2 Nitrate dynamics in the salinized rivers and the corresponding estuaries

290 4.2.1 Nitrate dynamics in the HH River and its estuary

291 A mixing line (HH1-E) was setup between the most upstream sampling location in the
292 HH River and the most downstream sampling location in the HH Estuary (Fig. 3).
293 After the separation of the floodgate F1, the upstream of the HH River serves as a
294 river-type reservoir. Thus, a new mixing line (HH2-E mixing line) was re-calculated
295 between the sampling location after the floodgate and estuarine water (Fig. 3). The
296 salinity gradient sampled in the HH River and its estuary showed a seaward
297 decreasing trend in DIN (NH_4^+, NO_2^- and NO_3^-) concentrations and an increasing
298 trend in $\delta^{15}N\text{-}NO_3^-$ and $\delta^{18}O\text{-}NO_3^-$ values throughout the entire salinity gradient (Fig.
299 3). However, the DIN and isotopic trends did not behave conservatively, as most of
300 the measured data deviated from the calculated mixing lines.

301 It is clear that in the upstream part of the HH River before the floodgate F1, NO_2^- and

NH_4^+ were above (a source) while NO_3^- was below (a sink) the HH1-E mixing line. Normally, the reductive removal of NO_3^- due to denitrification and assimilation is accompanied with N and O isotope fractionations. The kinetic isotope effects are responsible for preferentially utilizing the lighter isotopes ^{14}N and ^{16}O, causing an enrichment of the heavy isotopes in the remaining NO_3^- (Mariotti et al., 1981; Mayer et al., 2002; Fukada et al., 2003). Some studies reported that a linear relationship indicating an enrichment of ^{15}N relative to ^{18}O by a factor between 0.8 and 2.0 gives evidence for denitrification (Aravenaand and Robertson, 1998; Fukada et al., 2003; Xue et al., 2009) and 1.0 for assimilation (Granger et al. 2004). In our study, the ratio of N and O isotopic enrichment is 0.8, apparently implying that the removal process of NO_3^- in this river was predominated by denitrification rather than assimilation. From another aspect, elevated NH_4^+ compared to NO_3^- will inhibit NO_3^- assimilation by phytoplankton (Dugdale and Hopkins, 1978; Dugdale and MacIsaac, 1971; Dugdale et al., 2006), thus assimilation process is unlikely significant. The linear relation between the isotopic values and the logarithm of residual NO_3^- indicated that denitrification with constant enrichment factors (ε = -1.8‰ for $\delta^{15}N$ and ε = -1.4‰ for $\delta^{18}O$) was responsible for the increases in $\delta^{18}O$ and $\delta^{15}N$ as well. The relatively small enrichment factors were potentially linked to sedimentary denitrification, as diffusion limits the effects of fractionations in the sediments on the $\delta^{15}N$- and $\delta^{18}O$ NO_3^- in the overlying water column (Sebilo et al., 2003, Lehmann et al., 2004; Sigman et al., 2005). The NH_4^+ species was accumulated as a source, potentially originating from organic matter decomposition not sewage discharge, as the $\delta^{15}N$-NO_3^- values (-0.2-1.1‰) were out of the sewage range. Denitrification could also be the potential process for NO_2^- accumulation in the upstream part of the HH River. However, nitrification can not be excluded, especially at relatively low DO levels which may

327 favor ammonium oxidizers ($NH_4^+ \rightarrow NO_2^-$) rather than nitrite oxidizers ($NO_2^- \rightarrow NO_3^-$),
328 promoting NO_2^- accumulation (Helder and De Vries, 1998).
329 For the HH2-E mixing line after the floodgate F1 (Fig. 3), salinity gradient sampled in
330 the downstream of the HH River illustrated NO_3^- turned from a source (above the
331 HH2-E mixing line) to a sink (below the HH2-E mixing line), while NO_2^- and NH_4^+
332 turned from a sink (below the HH2-E mixing line) to a source (above the HH2-E
333 mixing line) at the end of the river. Nitrate accumulation may be linked to an
334 in-stream nitrification process, in which NO_2^- and NH_4^+ were consumed to produce
335 NO_3^-. In nitrification, the conversion of NH_4^+ to NO_2^- and NO_3^- is accompanied by
336 marked N isotope fractionation effects, resulting in ^{15}N depleted NO_3^- (Delwiche and
337 Steyn, 1970; Mariotti et al., 1981; Macko and Ostrom, 1994). For $\delta^{18}O\text{-}NO_3^-$ values,
338 NO_3^- produced by nitrification in aquatic environments usually takes similar $\delta^{18}O$
339 values to the ambient water (Casciotti et al. 2002; Sigman et al.2005). There is
340 evidence that O can exchange between H_2O and intermediate compounds of
341 nitrification (Andersson et al., 1982; DiSpirito and Hooper, 1986; Kool et al., 2007).
342 Since the $\delta^{18}O$ of estuarine water is expected to be higher than that of river water
343 (Miyajima et al., 2009), $\delta^{18}O\text{-}NO_3^-$ should increase along the salinity gradient when in
344 situ nitrification is occurring. Thus, a decrease in $\delta^{15}N$- (4.6-3.9‰) and an increase in
345 $\delta^{18}O\text{-}NO_3^-$ (0.6-1.2‰) occurred downstream of the HH River and confirmed the
346 in-stream nitrification process as a NO_3^- source. The NH_4^+ concentrations increased at
347 the end of the HH River (a maximum turbidity zone), probably from the release of
348 particle-bound NH_4^+ (Seitzinger et al., 1991; Schlarbaum et al., 2010). Results
349 (Kranck, 1984; Eisma, 1986; Schlarbaum et al., 2010) have been reported that this
350 NH_4^+ could originate from the mineralization of ^{15}N-enriched DON adsorbed onto the
351 particles and was released with the estuarine turbidity maximum. The ^{15}N-enriched

352 NH_4^+ was further converted to ^{15}N-enriched NO_3^-. Thus, the $\delta^{15}N$- NO_3^- increased
353 sharply from 3.9 to 8.4‰ while the $\delta^{18}O$- NO_3^- only increased slightly from 1.2 to
354 1.5‰, resulting from taking similar $\delta^{18}O$ values to the ambient water. Another
355 candidate reason to cause a sharp increase in NH_4^+ concentration could be sewage
356 discharge. Sewage is enriched in ^{15}N relative to other N sources, as ammonia
357 volatilization causes a large enrichment of ^{15}N in the residual NH_4^+. This NH_4^+ is
358 subsequently converted into ^{15}N-enriched NO_3^-. When salinity achieves 5, nitrifying
359 bacterial was potentially inhibited and reduced the conversion rate from NO_2^- to NO_3^-
360 (Pollice et al., 2002). Hence, the NO_2^- was accumulated and NO_3^- was declined in this
361 zone.
362 The DIN concentrations and $\delta^{15}N$- and $\delta^{18}O$-NO_3^- in the coastal water behaved
363 conservatively of a mixing. Since the separation of the floodgate F2 at the end of the
364 HH River, the salinity demonstrated a sudden increase from 4.9 (before the floodgate)
365 to 18.6 (after the floodgate) in 1 km, potentially indicate that the HH river discharge
366 was limited due to the floodgate F2. As the $\delta^{15}N$-NO_3^- value of the last sampling
367 location in the HH River was close to that of the estuarine water, hence $\delta^{15}N$-NO_3^-
368 values remained stable at ~8.0‰. The $\delta^{18}O$-NO_3^- values increase sea-ward because of
369 the high percentage of coastal water.
370
371 4.3 Nitrate dynamics in the CB River and JY River and their estuary
372 Compared to the HH River, the salinity of the CB and JY rivers varied in a relatively
373 small range, from 0.5 to 0.6 for the CB River and from 0.6 to 0.8 for the JY River.
374 Mixing lines were calculated between the CB and JY rivers and the estuarine water,
375 respectively (Fig. 4). Both CB and JY rivers demonstrated a NO_3^- source along the
376 salinity gradient, indicating a NO_3^- input from either in-stream nitrification or external

loading.

Nitrate concentrations in the CB River were elevated with a continuous accumulation along the river. The CB River flows through a rural area with intensive livestock production, likely resulting in NO_3^- contamination in the CB River (Shao et al., 2010). Furthermore, a regular source-sink pattern was observed for NH_4^+ concentrations while a decrease for NO_2^-. The sharp increase in NH_4^+ concentrations was probably linked to manure discharge in the rural area. The added NH_4^+ was then rapidly oxidized to NO_2^- and NO_3^- during nitrification. Hence, $\delta^{15}N\text{-}NO_3^-$ values were enriched and varied around 13.6‰, indicating NO_3^- derived from manure (Kendall et al., 2007; Xue et al., 2009). As NO_3^- from these origins is produced via nitrification, its $\delta^{18}O$ values would not be very different from ambient water. Thus, the gradual increase in $\delta^{18}O\text{-}NO_3^-$ values along the salinity gradient above the respected mixing line confirmed the in situ nitrification (see the discussion above). Thus, in the CB River, the NO_3^- turnover is mainly regulated by nitrification from external livestock N loadings.

The JY River became a significant source for NO_3^- in concert with a sink for NO_2^- and NH_4^+ species. The accumulation of NO_3^- was linked to the in-stream nitrification, resulting from the consumption of NO_2^- and NH_4^+. Evidence for this may be indicated by decreasing $\delta^{15}N\text{-}NO_3^-$ and increasing $\delta^{18}O\text{-}NO_3^-$ values along the river.

The salinity gradient sampled in the corresponding estuary showed a sea-ward decreasing trend in NH_4^+, NO_2^- and NO_3^- concentrations. The measured data in the CJ Estuary were expected to fall between the two calculated mixing lines generated from the rivers of CB and JY, because they both discharge into the same estuary. A major DIN source (above the two calculated mixing lines) appeared in the salinity zone between 2.0 and 4.2. This was probably from sewage discharge of mooring ships in

the vicinity of the sampling area. The typically high $\delta^{15}N\text{-}NO_3^-$ (13.6 to 15.0‰) values confirmed NO_3^- derivation from sewage. This point-source contamination was diluted by the estuarine water when salinity higher than 4.2, where the DIN concentrations and $\delta^{15}N\text{-}NO_3^-$ values fall between the two mixing lines. The $\delta^{18}O\text{-}NO_3^-$ values of the estuarine water were quite close to the $\delta^{18}O\text{-}NO_3^-$ derived from the nitrification of sewage, thus $\delta^{18}O\text{-}NO_3^-$ values were expected to retain stable.

4.4 Nitrate removal efficiency in the rivers and the estuaries

In this study, most of the measured data deviated from the calculated mixing lines, indicating rivers and estuaries becoming either a source or a sink. Thus, variation percentages of the measured data compared to the calculated mixing lines were computed to assess the NO_3^- removal efficiency for the rivers and estuaries (Fig. 5). Interestingly, in the upstream part of the HH River before the floodgate F1, NO_3^- was removed 30.9±22.1% compared to the calculated mixing line. Denitrification could be the dominant NO_3^- removal process. This potentially results from the separation of the floodgate F1 which limited water exchange with downstream water enriched in DO. Furthermore, the floodgate F1 might prolong water residence time in the upstream part to remove a significant part of riverine N loading. The downstream part of the HH River between floodgate F1 and floodgate F2 showed an extremely weak NO_3^- removal tendency (remove 2.5±13.3% of NO_3^-) from active NO_3^- turnover processes and the HH Estuary demonstrated a conservative behavior with respect to NO_3^-. In contrast, a significant source of NO_3^- is present in the CB (36.6±25.2%) and JY (34.6±35.1%) rivers compared to the calculated mixing line, explained by external N source addition and in-stream nitrification, respectively. Moreover, the CJ Estuary demonstrated higher NO_3^- accumulation efficiency (82.1±78.8%) as a result of an

external N source input. Great variation percentages were observed between the sampling points from the same river or estuary, possibly resulting from different N dynamics and/or external source input.

Estuaries of rivers are considered as active sites of massive NO_3^- losses (Brion et al., 2004; Seitzinger et al., 2006), removing up to 50% of NO_3^- (OsparCom, 2000). However, our data do not support this view as in the HH and the CJ Estuary. First, DO concentrations were higher than 10 mgL^{-1} not favorable for water column NO_3^- removal processes. Second, dredging and diking work to deepen the ship channel decreased the sediment area (where denitrification mainly occurred) that is in contact with the overlying water column in the rivers (Dähnke et al., 2008), thus the NO_3^- removal ability was reduced. Third, water residence time is not long enough to remove N loads in the estuaries by NO_3^- removing processes as reclamation projects for the regional and national economy leading to the hydrodynamics of circulation in Tianjin section disappearance (Qin et al., 2012). This phenomenon could reduce water residence time and force NO_3^- pollutants moving to the northern part of Bohai Bay, aggravating NO_3^- contamination.Furthermore, this wintertime situation, with water temperature around 10˚C, ruled out most biological activity, and conservative mixing behavior in the HH River Estuary was not overly surprising. However, the CJ Estuary became a NO_3^- source, linking to sewage discharge of mooring ships.

5. Conclusions

The combined use of salinity, DIN concentrations and NO_3^- isotopic composition revealed NO_3^- sources and dynamics in the salinized rivers of HH, CB and JY and elucidated mixing patterns of NO_3^- in the corresponding estuarine system. The HH River demonstrated a significant NO_3^- sink appeared in the upstream part of the HH

River by denitrification process. This potentially results from the separation of the floodgate F1 which limited water exchange with downstream water enriched in DO and prolong water residence time in the upstream to remove a significant part of riverine N loading. The downstream of the HH River showed an extremely weak NO_3^- removal tendency from active NO_3^- turnover processes. In contrast, a significant source of NO_3^- is present in the rivers of CB and JY, linking to external N source addition and in-stream nitrification, respectively. We found that the estuarine mixing behavior is mostly conservative excluding the point source input appeared in the CJ estuary. Data indicate that the rivers and their corresponding estuaries have lost their natural capacity of NO_3^- removal but turned into a significant source of NO_3^- for the adjacent Bohai Bay.

Acknowledgements: We gratefully acknowledge Xi Yang and Qing Chen for water sample preparation and the UC Davis Stable Isotope Facility of California University for isotope analyses. This study was financially supported by the National Science & Technology Pillar Program of China (2012BAC07B02), the National Natural Science Foundation of China (41203001; 41173096) and NCET Program (NCET-10-0954).

502 References

503 Andersson, K.K., Philson, S.B., Hooper, A.B., 1982. 18O isotope shift in 15N NMR
504 analysis of biological N-oxidations: H2O-NO2- exchange in the ammonia-oxidizing
505 bacterium Nitrosomonas. Proc. Natl. Acad. Sci. 79, 5871-5875.

506 Aravena, R., Robertson, W.D., 1998. Use of multiple isotope tracers to evaluate
507 denitrification in ground water: study of nitrate from a large-flux septic system
508 plume. Ground Water 36, 975-982.

509 Bernhardt, E.S., Likens, G.E., Buso, D.C., Driscoll, C.T., 2003. Instream uptake
510 dampens effects of major forest disturbance on watershed nitrogen export. Proc.
511 Natl. Acad. Sci. USA 100, 10304-10308.

512 Brion, N., Baeyens, W., De Galan, S., Elskens, M., Laane, R., 2004. The North Sea:
513 Source or sink for nitrogen and phosphorus to the Atlantic Ocean? Biogeochemistry
514 68, 277–296.

515 Casciotti, K.L., Sigman, D.M., Galanter Hastings, M., Böhlke, J.K., Hilkert, A. A.,
516 2002. Measurement of the oxygen isotopic composition of nitrate in seawater and
517 freshwater using the denitrifier method. Anal. Chem. 74: 4905-4912.

518 Chai, C., Yu, Z.M., Shen, Z.L., Song, X., Cao, X., Yao, Y., 2009. Nutrient
519 characteristics in the Yangtze River estuary and the adjacent east china sea before
520 and after impoundment of the Three Gorges Dam. Sci. Total Environ. 407,
521 4687–4695.

522 Chen, L., Li, J.., Guo, X., Fu, B., Li, G., 2000. Temporal and spatial characteristics of
523 surface water quality in Jiyun River. Environmental Science 21, 61-64. (In Chinese)

524 Dafner, E.V., Mallin, M.A., Souza, J.J., Wells, H.A., Parsons, D.C., 2007. Nitrogen
525 and phosphorus species in the coastal and shelf waters of Southeastern North
526 Carolina, Mid-Atlantic U.S. coast. Marine Chemistry 103, 289–303.

527 Dähnke K., Bahlman, E., Emeis, K., 2008. A nitrate sink in estuaries? An assessment
528 by means of stable nitrate isotopes in the Elbe estuary. Limnol. Oceanogr. 53,
529 1504-1511.
530 Dai, M., Wang, L., Guo, X., Zhai, W., Li, Q., He, B., Kao, S.J., 2008. Nitrification and
531 inorganic nitrogen distribution in a large perturbed river/estuarine system: the Pearl
532 River Estuary, China. Biogeosciences 5, 1227-1244.
533 Delwiche, C., Steyn, P., 1970. Nitrogen isotope fractionation in soils and microbial
534 reactions. Environ. Sci. Technol. 4, 929-935.
535 DiSpirito, A.A., Hooper, A.B., 1986. Oxygen exchange between nitrate molecules
536 during nitrite oxidation by Nitrobacter. Biol. Chem. 261, 10534-10537.
537 Dugdale, R.C., Hopkins, T.S., 1978. Predicting the structure and dynamics of a
538 pollution-driven marine ecosystem embedded in an oligotrophic sea. Thalassia
539 Jugoslavica 14, 107-126.
540 Dugdale, R.C., MacIsaac, J.J., 1971. A computational model for the uptake of nitrate
541 in the Peru upwelling region. Investigacion Pesquera 35, 299-308.
542 Dugdale, R.C., Wilkerson, F.P., Marchi, A., Hogue, V., 2006. Nutrient controls on new
543 production in the Bodega Bay, California, coastal upwelling plume. Deep-Sea
544 Research II 53, 3049-3062.
545 Eisma, D., 1986. Flocculation and de-flocculation of suspended matter in estuaries.
546 Fry, B., 2002. Conservative mixing of stable isotopes across estuarine salinity
547 gradients: A conceptual framework for monitoring watershed influences on
548 downstream fisheries production. Estuaries 25, 264-271.
549 Fukada, T., Hiscock, K.M., Dennis, P.F., Grischek, T., 2003. A dual isotope approach
550 to identify denitrification in ground water at a river bank infiltration site. Water Res.
551 37, 3070-3078.

552 Gao, X., Meng, H., Yi, X., 2011. Analysis of nitrogen pollution characteristics in
553 water bodies of Tianjin. China Water & Wastewater (in Chinese) 27, 51-55.
554 Gburek, W.J., Sharpley, A.N., 1998. Hydrology control on phosphorus loss from
555 upland agricultural watersheds. J. Environ. Qual. 270, 253-272.
556 Graas, S., Savenije, H.H.G., 2008. Salt intrusion in the Pungue estuary, Mozambique:
557 Effect of sand banks as a natural temporary salt intrusion barrier. Hydrol. Earth Syst.
558 Sci. Discuss. 5, 2523-2542.
559 Granger, J., Sigman, D.M., Needoba, J.A., Harrison, P.J., 2004. Coupled nitrogen and
560 oxygen isotope fractionation of nitrate during assimilation by cultures of marine
561 phytoplankton. Limnol. Oceanogr. 49, 1763-1773.
562 Hartzell, J.L., Jordan, T.E., 2012. Shifts in the relative availability of phosphorus and
563 nitrogen along estuarine salinity gradients. Biogeochemistry 107, 489–500.
564 Helder, W., De Vries, R.T.P., 1983. Estuarine nitrite maxima and nitrifying bacteria
565 (Ems-Dollard estuary). Netherlands Journal of Sea Research 17, 1–18.
566 Jennerjahn, T.C., Ittekkot, V., Klöpper, S., Adi, S., Nugroho, S.P., Sudiana N., Yusmal,
567 A., Prihartanto, Gaye-Haake. B., 2004. Biogeochemistry of a tropical river affected
568 by human activities in its catchment: Brantas river estuary and coastal waters of
569 Madura Strait, Java, Indonesia. Estuar. Coast. Shelf Sci. 60, 503-514.
570 Kendall, C., Elliott, E.M., Wankel, S.D., 2007. Tracing anthropo- genic inputs of
571 nitrogen to ecosystems. In: Stable isotopes in ecology and environ- mental science,
572 eds. Michener, R., Lajtha, K., pp 375-449. Blackwell, Maiden.
573 Kool, D.M., Wrage, N., Oenema, O., Dolfing, J., Van Groenigen, J.W., 2007. Oxygen
574 exchange between (de)nitrification intermediates and H2O and its implication for
575 source determination of NO3- and N2O: a review. Rapid Commun. Mass Spectrom.
576 21, 3659-3578.

577 Kranck, K., 1984. Role of flocculation in the filtering of particulate matter in
578 estuaries.In: Kennedy, V.S. (Ed.), The Estuary as a Filter. New York, Academic
579 Press, Orlando FL., pp. 159–175.
580 Lehmann, M.F., Sigman, D.M., Berelson, W.M., 2004. Coupling the 15N/14N and
581 18O/16O of nitrate as a constraint on benthic nitrogen cycling. Marine Chemistry 88,
582 1–20.
583 Liang, Y., Xing, H., 1999. Preliminary analysis of the characteristics of tidal dynamic
584 and sediment at the Yongdingxinhe River Mouth. Haihe Water Resources (in
585 Chinese) 2, 13-15.
586 Liss, P.S., 1976. Conservative and non-conservative behavior of dissolved
587 constituents during estuarine mixing. In Estuarine chemistry, eds. Burton, J.D., Liss,
588 J.D., pp. 93-130. Academic press.
589 Liu, G., Fu, B., Yang, P., 2001. Quality of aquatic environment at Haihe River and the
590 pollutant fluxes flowing into sea. Environmental Science (in Chinese) 22, 46-50.
591 Macko, S.A., Ostrom, N.E., 1994. Molecular and pollution studies using stable
592 isotope. In: Stable Isotopes in Ecology and Environmental Science, eds. Lajtha, K.,
593 Michner, R., pp. 45-62. Blackwell Scientific, Oxford, UK.
594 Mariotti, A., Germon, J.C., Hubert, P., Kaiser, P., Letolle, R., Tardieux, A., Tardieux,
595 P., 1981. Experimental determination of nitrogen kinetic isotope fractionation: some
596 principle illustration for the denitrification and nitrification processes. Plant Soil 62,
597 413-430.
598 Mayer, B., Boyer, E.W., Goodale, C., Jaworski, N.A., Breemen, N.V., Howarth, R.W.,
599 Seitzinger, S., Billen, G., Lajtha, K., Nadelhoffer, K., Dam, D.V., Hetling, L.J.,
600 Nosal, M., Paustian, K., 2002. Sources of nitrate in rivers draining sixteen
601 watersheds in the northeastern U.S.: Isotopic constraints. Biogeochemistry 57/58,

171-197.

Middelburg, J.J., Herman, P.M.J., 2007. Organic matter processing in tidal estuaries. Marine Chemistry 106,127–147.

Middelburg, J.J., Nieuwenhuize, J., 2001. Nitrogen isotope tracing of dissolved nitrogen behavior in tidal estuaries. Estuar. Coast. Shelf Sci. 53, 385-391.

Miyajima, T., Yoshimizu, C., Tsuboi, Y., Tanaka, Y., Tayasu, I., Nagata, T., Koike, I., 2009. Longitudinal distribution of nitrateδ15N andδ18O in two contrasting tropical rivers: implications for instream nitrogen cycling. Biogeochemistry 95, 243-260.

Mulholland, P.J., 1992. Regualtion of nutrient concentrations in a temperate forest stream: roles of upland, riparian, and instream processes. Limnol. Oceanogr. 37, 1512-1526.

Neth. J. Sea Res. 20, 183–199.

OSPARCOM. 2000. Quality Status Report 2000, Region II – Greater North Sea. OSPAR Commission. 136+ xiii p.

Pollice A., Tandoi V., Lestingi C., 2002. Influence of aeration and sludge retention time on ammonium oxidation to nitrite and nitrate. Water Res. 36, 2541- 2546.

Qin, Y.,Zhange, L., Zheng, B., Cao, W., Liu, X., Jia, J., 2012. Impact of shoreline changes on the costal water quality of Bohai Bay (2003-2011). Acta Scientiae Circumstantiae (in Chinese) 32, 2149-2159.

Rabalais, N.N., Turner, R.E., JustiĆ, D., Dortch, Q., Wiseman, W.J., Sen Gupta, B.K., 1996. Nutrient Changes in the Mississippi River and System Responses On the Adjacent Continental Shelf. Estuaries 19, 386–407.

Schlarbaum, T., Daehnke, K., Emeis, K., 2010. Turnover of combined dissolved organic nitrogen and ammonium in the Elbe estuary/NW Europe: Results of nitrogen isotope investigations. Marine chemistry 119, 91-107.

627 Sebilo, M., Billen, G., Grably, M., Mariotti, A., 2003. Isotopic composition of
628 nitrate-nitrogen as a marker of riparian and benthic denitrification at the scale of the
629 whole Seine River system. Biogeochemistry 63, 35–51.
630 Sebilo, M., Billen, G., Mayer, B., Billiou, D., Grably, M., Garnier, J., Mariotti, A.,
631 2006. Assessing nitrification and denitrification in the Seine River and Estuary
632 using chemical isotopic techniques. Ecosystems 9, 564-577.
633 Seitzinger, S., Gardner, W.S., Spratt, A.K., 1991. The effect of salinity on ammonia
634 sorption in aquatic sediments: implications for benthic nutrient recycling, Estuaries
635 2, 167-174.
636 Seitzinger, S., Harrison, J.A., Böhlke, J.K., Bouwman, A.F., Lowrance, R., Peterson,
637 B., Tobias, C., Van Drecht, G.., 2006. Denitrification across landscapes and
638 waterscapes: A synthesis. Ecol. Appl. 16, 2064–2090.
639 Seitzinger, S.P., Kroeze, C., 1998. Global distribution of nitrous oxide production and
640 N inputs in freshwater and coastal marine ecosystems. Glob. Biogeochem. Cycles
641 12, 93-113.
642 Shao, X., Deng, X., Yuan, X., Jiang, W., 2010. Identification of potential sensitive
643 areas of non- point source pollution in downstream watershed of Chaobaixin River.
644 Environmental Science Survey (in Chinese) 29, 37-41.
645 Sigman, D.M., Casciotti, K.L., Andreani, M., Barford, C., Galanter, M., Böhlke, J.K.,
646 2001. A bacterial method for the nitrogen isotopic analysis of nitrate in seawater
647 and freshwater. Anal. Chem. 73: 4145-4153.
648 Sigman, D.M., Granger, J., DiFiore, P.J., Lehmann, M.L., Ho, R., Cane, G., Van Geen,
649 A., 2005. Coupled nitrogen and oxygen isotope measurements of nitrate along the
650 eastern North Pacific margin. Global Biogeochem. Cycl. 19, GB4022.
651 Umezawa, Y., Hosono, T., Onodera, S., Siringan F., Buapeng, S., Delinom, R.,

652 Yoshimizu, C., Tayasu, I., Nagata, T., Taniguchi, M., 2008. Sources of nitrate and
653 ammonium contamination in groundwater under developing Asian megacities. Sci.
654 Total. Environ. 404, 361-376.
655 Wang, L., 2004. A discussion on the deep fresh water salinization in the plain region
656 of Tianjin City. Geological Survey and Research (in Chinese) 27, 169-176
657 Wankel, S.D., Kendall, C., Francis, C.A., Paytan, A., 2006. Nitrogen sources and
658 cycling in the San Francisco Bay Estuary: A nitrate dual isotopic composition
659 approach. Limnol. Oceanogr. 51, 1654-1664.
660 Wen, S., Xing, H., 2004. The characteristics of water and sand in the Haihe River
661 estuary and movement rule analysis. Haihe Water Resources (in Chinese) 2, 28-31.
662 Xue, D., Botte, J., De Baets, B., Accoe, F., Nestler, A., Taylor, P., Van Cleemput, O.,
663 Berglund, M., Boeckx, P., 2009. Present limitations and future prospects of stable
664 isotope methods for nitrate source identification in surface- and groundwater. Water
665 Res. 43, 1159–1170.
666 Xue, D., De Baets, B., Vermeulen, J., Botte, J., Van Cleemput, O., Boeckx, P., 2010.
667 Error assessment of nitrogen and oxygen isotope ratios of nitrate as determined via
668 the bacterial denitrification method. Rapid Commun. Mass Spectrom. 24:
669 1979-1984.
670 Yue, F., Liu, X., Li, J., Zhu, Z., Wang, Z., 2010. Using nitrogen isotopic approach to
671 identify nitrate sources in waters of Tianjin, China. Bull. Environ. Contam. Toxicol.
672 85, 562-567.
673 Zhang, J.,Yu, Z.G., Raabe, T., Liu, S., Starke, A., Zou, L., Gao, H., Brockmann, U.,
674 2004. Dynamaics of inorganic nutrient species in the Bohai seawaters. J. Mar. Syst.
675 44, 189-212.
676
677

678 Table 1. Physicochemical properties and isotopic composition of NO_3^- for the three investigated rivers and the corresponding estuaries.

Location	Salinity (‰)	pH	T (˚C)	DO (mg L^{-1})	NO_2^-	NO_3^-	NH_4^+	$\delta^{15}N\text{-}NO_3^-$	$\delta^{18}O\text{-}NO_3^-$
					————μ mol L^{-1}————			——‰——	
HH*	0.7	7.5	11.4	2.7	16.6	219.0	221.4	-0.2	-0.5
	0.7	7.7	12.1	4.0	18.0	145.6	332.6	0.5	0.2
	0.7	7.7	12.2	4.8	18.6	134.4	311.3	0.6	0.2
	0.8	7.9	13.2	5.0	20.8	105.0	326.9	1.1	0.5
	1.0	8.1	13.1	8.2	10.0	94.7	157.9	4.5	0.6
	2.3	8.4	12.1	10.4	7.2	90.2	124.1	4.6	1.1
	2.4	8.5	11.9	10.5	8.6	94.0	127.1	4.3	1.3
	3.7	8.3	12.7	10.4	8.8	89.0	127.3	3.9	1.2
	4.6	8.3	12.1	9.9	15.5	62.5	156.8	8.4	1.5
	4.9	8.2	11.7	9.4	14.5	70.0	149.5	7.4	1.4
Average	2.2±1.7	8.1±0.3	12.3±0.6	7.5±3.1	13.9±4.8	110.4±45.9	203.5±87.5	3.5±3.0	0.8±0.7
HH&	18.6	8.2	10.1	10.7	6.7	25.7	88.1	8.0	5.4
	20.6	8.2	10.2	10.7	6.3	17.8	79.9	7.9	5.6
	21.3	8.1	9.6	10.7	6.2	15.1	76.9	8.1	5.7
	24.1	8.1	9.0	10.7	5.6	7.1	65.7	8.3	5.8
Average	21.2±2.3	8.2±0.1	9.7±0.6	10.7±0.0	6.2±0.5	16.4±7.7	77.7±9.3	8.1±0.2	5.6±0.2
CB*	0.5	7.9	11.3	8.9	12.0	120.0	333.4	13.7	4.0
	0.5	8.6	10.8	10.5	7.0	134.1	167.1	14.0	4.8
	0.5	8.5	10.7	9.1	10.6	157.8	380.0	13.9	3.9
	0.5	8.5	10.5	9.9	9.9	171.5	143.9	12.2	4.3
	0.6	8.6	11.0	10.4	6.0	171.1	367.0	13.7	4.8
	0.6	8.2	10.8	10.0	8.5	152.4	210.1	14.1	5.6
Average	0.5±0.1	8.4±0.3	10.9±0.3	9.8±0.7	9.0±2.3	151.2±20.6	266.9±105.4	13.6±0.7	4.6±0.6

Continued

JY*	0.6	8.1	9.9	7.2	7.0	40.0	72.8	6.5	0.9
	0.7	8.2	11.0	8.7	6.9	42.0	64.4	6.3	2.0
	0.7	8.2	11.3	7.5	4.4	44.0	57.6	6.4	1.4
	0.7	8.4	11.7	9.3	4.9	46.0	48.1	5.8	0.8
	0.8	8.4	12.4	9.3	4.0	76.6	12.7	5.3	1.3
	0.8	8.4	11.8	9.7	3.8	78.0	25.9	5.3	1.1
	0.8	8.5	11.8	9.9	2.2	83.3	11.1	4.4	2.8
	0.8	8.5	11.8	9.9	2.1	81.5	35.1	4.4	5.3
Average	0.7±0.1	8.3±0.2	11.5±0.8	8.9±1.1	4.4±1.8	61.4±19.9	41.0±23.4	5.6±0.8	2.0±1.5
CJ[&]	2.0	8.2	7.8	10.6	7.7	153.4	328.4	13.6	5.9
	2.5	8.2	6.9	11.4	7.8	120.0	304.7	15.0	6.1
	2.7	8.3	5.7	11.5	7.6	110.0	283.3	14.7	6.4
	4.2	8.3	5.7	11.1	7.0	130.0	286.3	13.6	6.4
	9.0	8.3	5.7	11.4	5.8	37.0	180.7	11.9	6.2
	13.7	8.3	6.2	11.3	4.9	24.0	120.4	9.3	6.7
	20.0	8.2	8.6	11.2	3.4	6.1	43.2	7.1	6.9
Average	7.7±6.9	8.3±0.1	6.7±1.2	11.2±0.3	6.3±1.7	82.9±58.8	221.0±108.0	12.2±3.0	6.4±0.3

* represents river; [&] represents estuary.

685 Figure Captions:

686 Fig. 1 Sampling locations for the three investigated rivers.

687 Fig. 2 $\delta^{15}N$ and $\delta^{18}O\text{-}NO_3^-$ of the salinized rivers and estuaries. Ranges of isotopic
688 composition for five potential NO_3^- sources are adapted from Kendall et al., (2007)
689 and Xue et al. (2009) and indicated by boxes: NO_3^- in precipitation (NP), NO_3^-
690 fertilizer (NF), NH_4^+ in fertilizer and rain (NFR), soil N (Soil) and manure and
691 sewage (M&S). To provide a range of $\delta^{18}O\text{-}NO_3^-$ values more wide and clear, the
692 upper limit of NP reaches 50‰.

693 Fig. 3 DIN (NH_4^+, NO_2^-, NO_3^-) concentrations and isotopic composition of NO_3^-
694 versus salinity in the HH River and the HH Estuary. HH1-E represented the calculated
695 mixing line between the initial upstream and the estuary; HH2-E represented the
696 calculated mixing line between the floodgate F1 and the estuary; F represents
697 floodgate.

698 Fig. 4 DIN (NH_4^+, NO_2^-, NO_3^-) concentrations and isotopic composition of NO_3^-
699 versus salinity in the CB River and the JY River and the CJ Estuary. CB-E represented
700 the calculated mixing line between the CB River and the CJ Estuary; JY-E represented
701 the calculated mixing line between the JY River and the CJ Estuary.

702 Fig. 5 Variation percentage compared to the calculated mixing lines for the HH River,
703 CB River, JY River and their corresponding estuaries of HH and CJ. When the
704 percentage >0 representing a source; when the percentage <0 representing a sink;
705 when the percentage equal to 0 representing a mixing; * represents a river.

706

707

708

709

710

711 Figure 1 Xue et al.

712

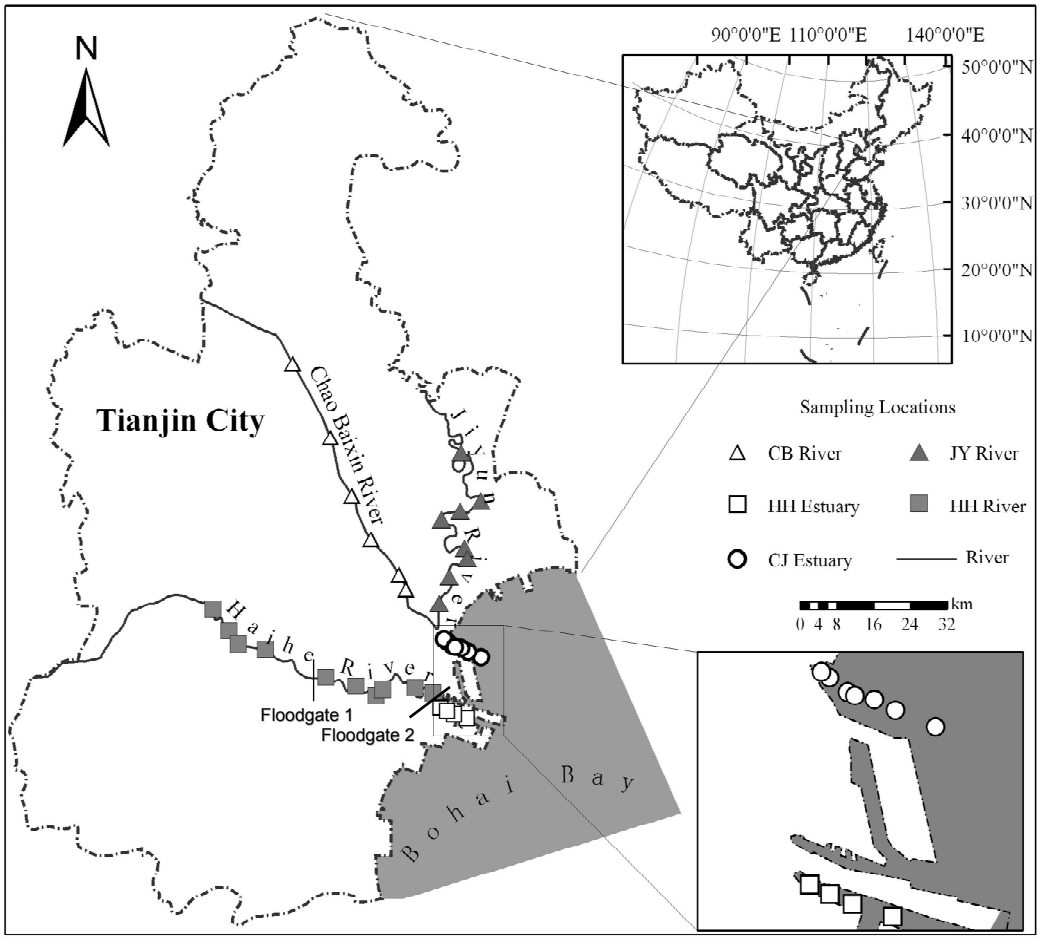

713

714

715

716

717

718

719

720

721

722

723

724

725

726

727

728 Figure 2 Xue et al.

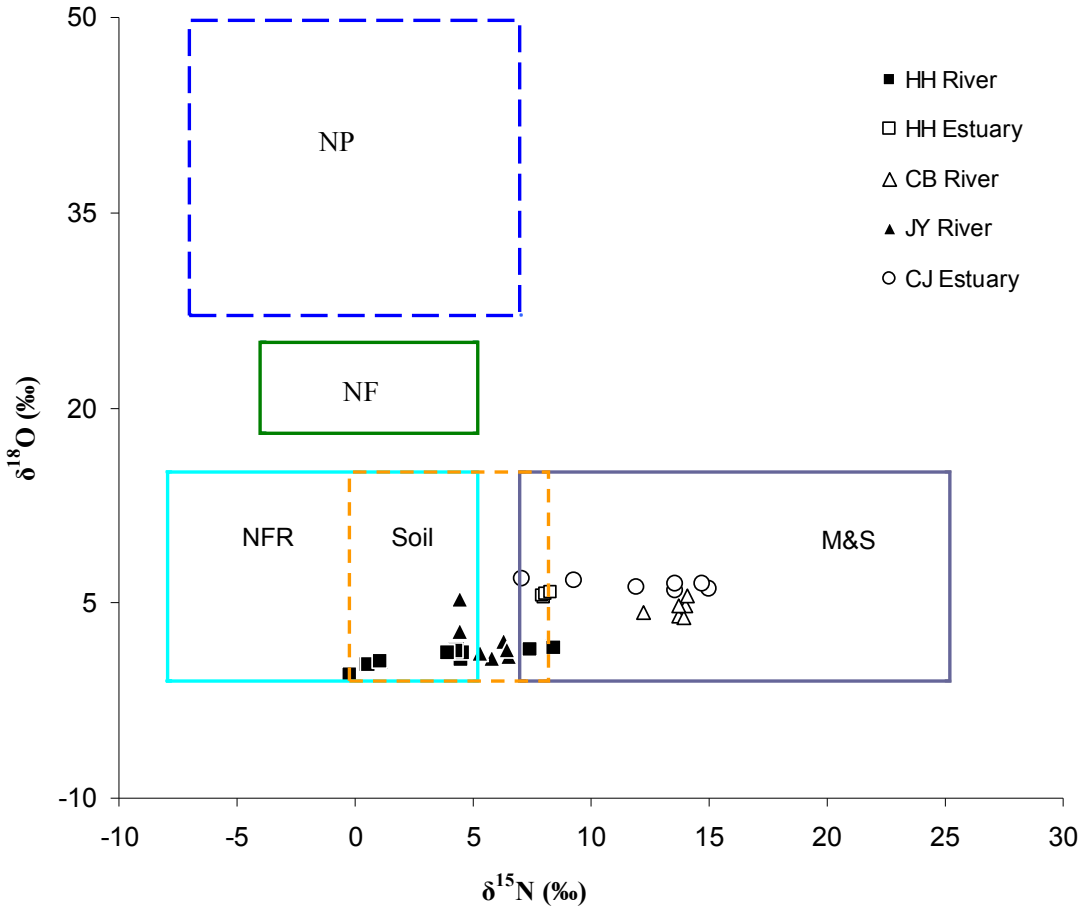

729
730
731
732
733
734
735
736
737
738
739
740
741
742
743
744

745 Figure 3 Xue et al.

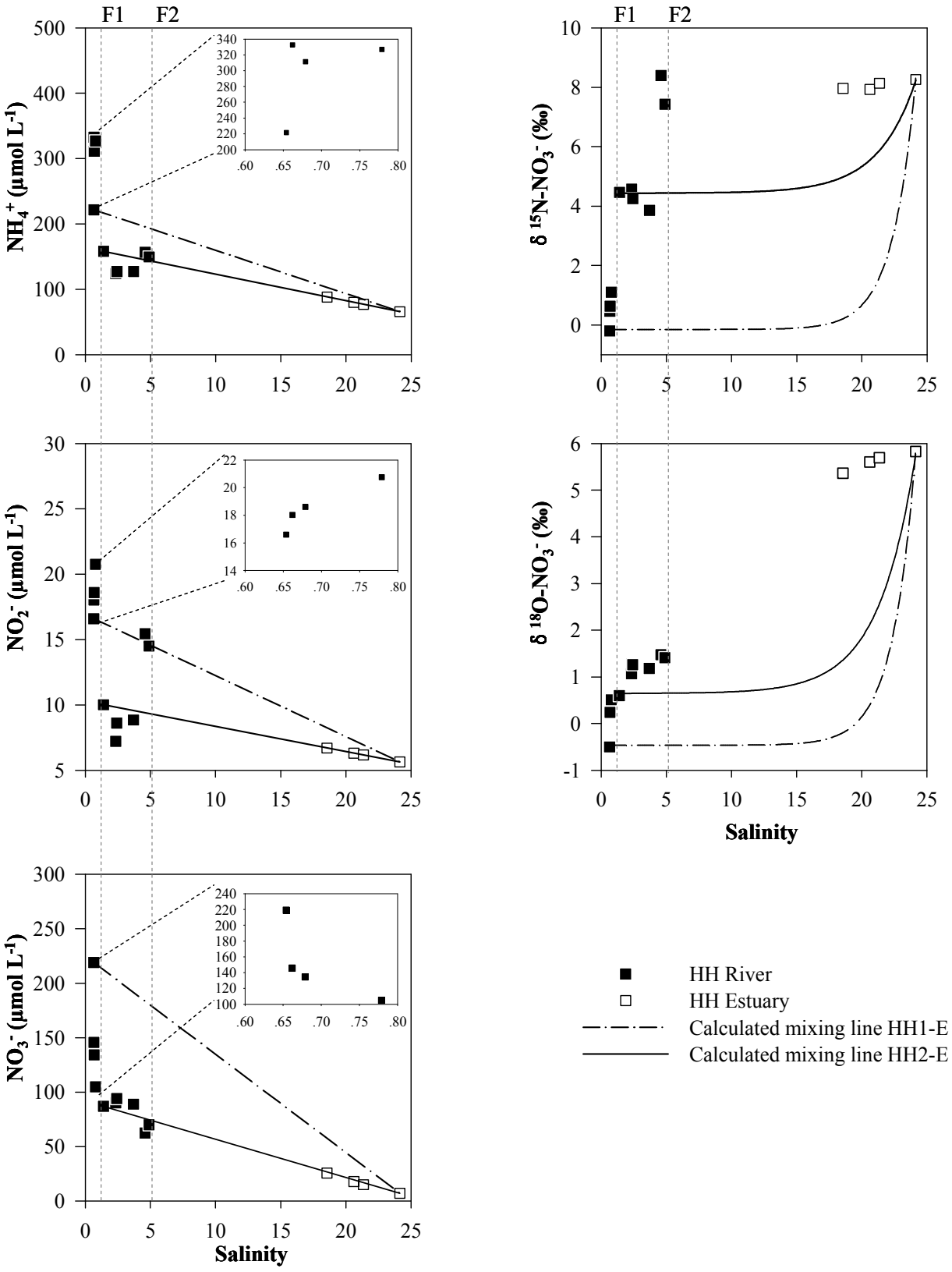

746

747

748

Figure 4 Xue et al.

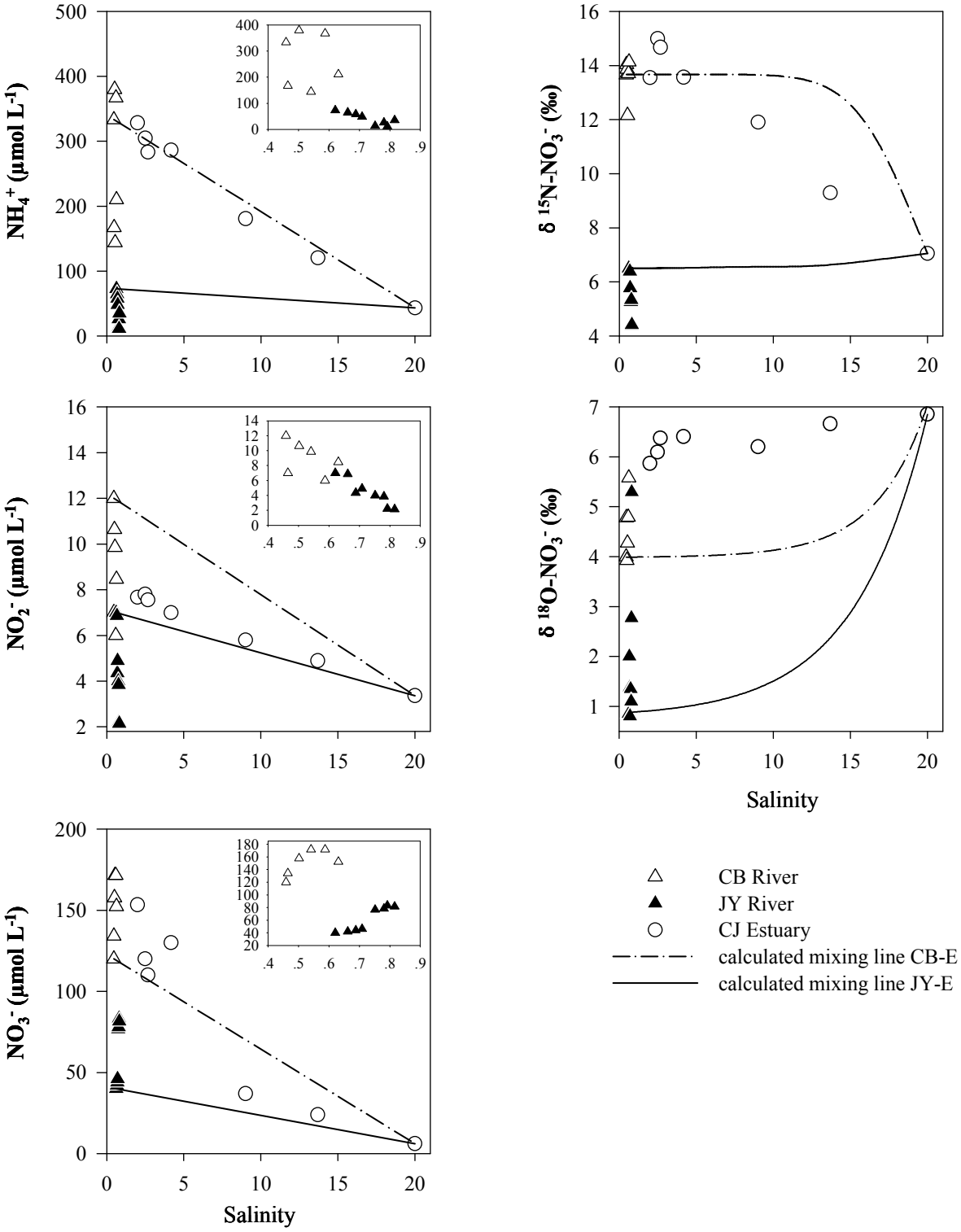

Figure 5 Xue et al.